ELSEVIER

Computational Geometry 21 (2002) 63–86

Computational Geometry
Theory and Applications

www.elsevier.com/locate/comgeo

Surface reconstruction using umbrella filters ☆

Udo Adamy *, Joachim Giesen, Matthias John

Institute for Theoretical Computer Science, ETH Zürich, Zürich, Switzerland

Communicated by M.J. Katz and K. Kedem; received 30 June 2000; received in revised form 17 February 2001; accepted 17 February 2001

Abstract

We present a new approach to surface reconstruction in arbitrary dimensions based on the Delaunay complex. Basically, our algorithm picks locally a surface at each vertex. In the case of two dimensions we prove that this method gives indeed a reconstruction scheme. In three dimensions we show that for smooth regions of the surface this method works well and at difficult parts of the surface yields an output well-suited for postprocessing. As a postprocessing step we propose a topological clean up and a new technique based on linear programming in order to establish a topologically correct surface. These techniques should be useful also for many other reconstruction algorithms.

Keywords: Surface reconstruction; Gabriel graph; Linear programming

1. Introduction

In general, the surface reconstruction problem asks for a piecewise linear reconstruction of a closed hypersurface in $\mathbb{R}^d$ that interpolates a given set S of sample points. The importance of the problem comes mainly from the three dimensional case, where many devices for finite samplings of surfaces exist, e.g. laser range scanners or contact probe digitizers. However, also the two dimensional case, that has applications in image processing, attracted several researchers.

Obviously, the set of sample points must be sufficiently dense to capture the various features of the surface. While smooth parts are relatively easy to reconstruct, in non-smooth parts of the surface even very dense samplings may not be sufficient to capture all features.

There are application domains where it is important to have not only a visually pleasing, but rather a topologically correct output of the reconstruction algorithm. This output might be used as input mesh for

☆ This work was supported by grants from the Swiss Federal Office for Education and Science (Projects ESPRIT IV LTR No. 21957 CGAL and NO. 28155 GALIA).

* Corresponding author.

E-mail addresses: adamy@inf.ethz.ch (U. Adamy), giesen@inf.ethz.ch (J. Giesen), john@inf.ethz.ch (M. John).

0925-7721/02/$ – see front matter
PII: S0925-7721(01)00040-2

finite element calculations. Furthermore, many methods for processing meshes, e.g. mesh compression or geometric modeling, rely on a topologically correct mesh.

1.1. Related work in three dimensions

In recent years, the surface reconstruction problem in three dimensions found some attraction from researchers in computer graphics as well as from researchers in computational geometry. This interest is mainly motivated by the pervasive availability of hardware devices to measure points on the surface of physical objects.

The problem was made popular by a paper of Hoppe et al. [20]. They presented an algorithm which reconstructs the surface as the zero set of a signed distance function. This approach is not able to capture fine features of the surface. It also does not interpolate but approximates the set of sample points. A related algorithm by Curless and Levoy [13] is capable to do so, but it relies on additional information than just the sample points.

Researchers from the computational geometry community based their algorithms on the Delaunay complex of the sample points. In three dimensions the Delaunay complex is a tetrahedralization of the point set. It is well studied and has found many applications over the years. Boissonnat [9] gave the first Delaunay based reconstruction algorithm that removes tetrahedra and triangles violating certain conditions from the Delaunay complex. Unfortunately, it applies only to surfaces of genus zero.

The α-complex is a subcomplex of the Delaunay complex and usually it is computed via the Delaunay complex. Edelsbrunner and Mücke [16] and Bajaj et al. [8] used α-shapes for surface reconstruction. Their algorithms are highly sensitive to the parameter α and work well only for samples of almost uniform density. Teichmann and Capps [22] introduced density scaled α-shapes to avoid the latter problem. However, their approach needs normals at the sample points.

Veltkamp [24] introduced the γ-graph, a generalization of the Delaunay complex, the Gabriel graph and the β-skeleton [21]. The γ-graph is suited for surface reconstruction by removing simplices from an initial complex similar to [9]. The technique of assigning γ-values to simplices is similar to our approach.

Amenta and Bern [3,5] presented the first algorithm with a theoretical guarantee. For sufficiently dense samplings their algorithm gives a piecewise linear surface which is homeomorphic and geometrically close to the original surface. However, for non-smooth surfaces Amenta and Bern were not able to give any guarantee. In fact their algorithm has difficulties reconstructing non-smooth or badly sampled parts of a surface properly. The *co-cone* algorithm of Amenta et al. [6] is an elegant and fast simplification of the algorithm of Amenta and Bern, which holds the same theoretical guarantee.

A drawback of all Delaunay based algorithms is that in practice their output need not be a topologically correct surface. All these algorithms consider candidate triangles from the Delaunay complex by some criterion. In practice these triangles are unlikely to form a topologically correct surface due to noise, undersampling or sharp surface features. Especially Attali [7] reports many missing triangles for her Delaunay based reconstruction algorithm.

Throughout this paper, we assume that the sample points are not associated with additional information, the sampling need not be uniform, the surface need not be smooth and is not restricted to any specific genus. A preliminary version of this paper appeared in [1].

1.2. Related work in two dimensions

A hypersurface in two dimensions is a simple closed curve. The correct reconstruction has to connect the sample points in the same order as they are connected along the curve. For curves, quite a lot of algorithms with provable guarantees are known, i.e., Amenta et al. [4] presented a two-dimensional version of their surface reconstruction algorithm as a precursor. All these algorithms are based on the two-dimensional Delaunay complex and can provably reconstruct smooth curves correctly. Our surface reconstruction algorithm can also be adapted to curves. This adaptation gives a provably correct reconstruction scheme for simple, closed and smooth curves.

The first algorithm capable of reconstructing non-smooth curves was given by Giesen [19]. He showed that the Traveling salesman tour is a reconstruction scheme for simple closed curves. Althaus and Mehlhorn [2] described a polynomial time implementation of Giesen's algorithm. Their implementation is based on linear programming and makes use of the fact that piecewise linear, simple closed curves can be characterized by a set of linear inequalities. In this paper we show that piecewise linear, compact surfaces without boundaries in three dimensions can also be characterized by a set of linear inequalities. We use these inequalities to handle non-smooth or undersampled parts of the surface we want to reconstruct.

In Section 2 we discuss some fundamental ideas. In Section 3 we describe our basic algorithm in arbitrary dimensions and specialize it to the two and three dimensional case. For the latter case we show how to enforce topological correctness of the output. In Section 4 we offer extensive experimental results and general discussion.

2. Subcomplexes of the Delaunay complex

The Delaunay complex of a finite set $S \subset \mathbb{R}^d$ is the collection of all Delaunay simplices with vertices in S. A subset $K \subseteq S$ with $|K| \leqslant d+1$ defines a Delaunay simplex, if there exists an open ball empty of points from S, that has all points of K in its boundary. The Delaunay simplex associated with K is just the convex hull of K. The Delaunay complex is a well studied data structure, especially in dimensions two and three, where many efficient and robust implementations exist, e.g. [10].

Many subcomplexes of the Delaunay complex have been proposed for surface reconstruction. Here we briefly recapitulate two such subcomplexes, namely α-shapes and β-skeletons.

The *α-shape* of a finite set $S \subset \mathbb{R}^d$ for $\alpha \in [0, \infty]$ was introduced by Edelsbrunner et al. [15] and proposed for reconstruction in [16]. For $k \leqslant d-1$, a k-simplex with vertices $v_0, \ldots, v_k$ belongs to the α-shape of S, iff there is an empty open ball b with radius α and $\partial b \cap S = \{v_0, \ldots, v_k\}$. In surface reconstruction we slightly abuse the notation and consider only $(d-1)$-simplices to belong to the α-shape.

The *β-skeleton* was introduced by Kirkpatrick and Radke [21]. For $\beta \geqslant 1$, the β-skeleton of a finite set $S \subset \mathbb{R}^d$ is the $(d-1)$-dimensional complex given by the following *forbidden region condition*. A $(d-1)$-simplex σ with vertices $v_0, \ldots, v_{d-1} \in S$ belongs to the β-skeleton of S, iff the union of the two d-dimensional balls tangent to $v_0, \ldots, v_{d-1}$ with diameter $\beta \cdot \operatorname{diam}(\sigma)$ is empty. Here $\operatorname{diam}(\sigma)$ denotes the diameter of the smallest d-dimensional ball which has $v_0, \ldots, v_{d-1}$ on its boundary.

Both concepts have their drawbacks in surface reconstruction. α-shapes cannot adapt to varying sampling density along the surface, since the global value α has to be chosen in such a way that it fits for the sparsest sampled parts of the surface. Such a value might not be adequate for densely sampled parts. In contrast to that, the β-skeleton adapts nicely to varying sampling densities, but the *forbidden region*

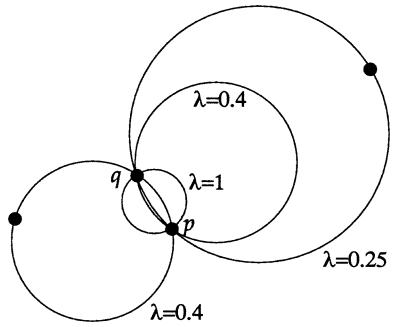

Fig. 1. Some λ-balls of the line segment $\overline{pq}$.

condition is more restrictive than the condition for α-shapes. Hence many simplices one wants to have in the reconstruction might not be in the β-skeleton. This is especially the case for non-smooth surfaces.

We want to combine the advantages and, at the same time, avoid the disadvantages of both concepts. The λ-complex of a finite set $S \subset \mathbb{R}^d$ is a complex that adapts to varying sampling density, but is not too restrictive. As above, for a $(d-1)$-simplex σ let $\operatorname{diam}(\sigma)$ be the diameter of the smallest circumscribed ball.

Given $\lambda \in (0, 1]$ and a simplex σ with vertices in the set S, a λ-ball $b_\lambda(\sigma)$ is an open d-dimensional ball with diameter $\operatorname{diam}(\sigma)/\lambda$ that has all vertices of σ on its boundary. For $\lambda = 0$, we define $b_\lambda(\sigma)$ to be an open halfspace through the vertices of σ. The λ-interval of a simplex is now defined as follows.

Definition 2.1 (λ-interval). The λ-interval $I(\sigma)$ assigned to a $(d-1)$-simplex σ with points in S is

$$I(\sigma) = \{\lambda\colon \exists b_\lambda(\sigma) \text{ with } b_\lambda \cap S = \emptyset\}.$$

Observe that for $(d-1)$-simplices σ in the Delaunay complex their λ-interval $I(\sigma)$ is a subinterval of $[0, 1]$, whereas simplices that are not in the Delaunay complex have empty λ-intervals.

The λ-complex for a given interval $I \subseteq [0, 1]$ consists of all $(d-1)$-simplices σ in the Delaunay complex of S for which the interval I is contained in the assigned λ-interval, i.e. $I \subseteq I(\sigma)$. The λ-complex for the degenerate interval $[1, 1]$ (containing only the point 1) is called the *Gabriel complex*. Intuitively, the λ-interval is a measure for the heterogeneity of the open balls that have the points of the $(d-1)$-simplex in its boundary and do not contain any sample point. Fig. 1 shows an example in dimension two.

The λ-interval of the line segment $\overline{pq}$ in Fig. 1 is $[0.25, 1]$ since for each $0.25 \leqslant \lambda \leqslant 1$ there exists a λ-ball empty of sample points and all λ-balls with $\lambda < 0.25$ contain a sample point. Observe that in general a small lower interval bound means that at least on one side of the simplex a large ball empty of sample points passes through this simplex. An upper bound of the interval smaller than 1 means that there are sample points close to the simplex.

The λ-interval $I(\sigma)$ of a $(d-1)$-simplex σ can be computed efficiently from the Delaunay complex of the sample points. Let σ_1 and σ_2 be the two d-dimensional simplices adjacent to σ in the Delaunay complex. If σ_i does not exist, i.e. σ is in the convex hull of the sample points S, set $\lambda_i = 0$, otherwise set

$$\lambda_i = \frac{\operatorname{diam}(\sigma)}{\operatorname{diam}(\sigma_i)}.$$

Note that in the two-dimensional case $\lambda_i = \sin\alpha_i$, where α_i is the angle in σ_i opposite to σ.

The lower bound of the λ-interval $I(\sigma)$ equals $\min\{\lambda_1, \lambda_2\}$. The upper bound of $I(\sigma)$ is given by 1, iff the centers of the circumscribed balls of σ_1 and σ_2 lie on different sides of the hyperplane through σ. Otherwise the upper bound equals $\max\{\lambda_1, \lambda_2\}$.

3. The algorithm UMBRELLAFILTER

Any point of a d-dimensional manifold has a neighborhood that is homeomorphic to the open ball $\mathbb{D}^d = \{x \in \mathbb{R}^d\colon\ |x| < 1\}$. We are dealing with piecewise linear manifolds, i.e. simplicial complexes satisfying a further condition, which we refer to as umbrella condition.

Definition 3.1 (Umbrella condition). The neighborhood of a vertex v in a d-dimensional simplicial complex K is the union of the interiors of all simplices in K incident to v together with the vertex v itself.

A complex is called surface complex, if the neighborhood of every point v is homeomorphic to the open ball $\mathbb{D}^d$. Such a neighborhood is called an umbrella.

The algorithm UMBRELLAFILTER chooses for every sample point an optimal umbrella from the Gabriel complex using the following optimality criterion. Choose the umbrella that minimizes the maximum of the lower λ-interval bounds of all its $(d-1)$-simplices. We compute both the λ-intervals and the Gabriel complex from the Delaunay complex. In pseudocode the algorithm reads as follows:

```
UMBRELLAFILTER (S ⊂ ℝ^d)
Compute the Delaunay triangulation DT(S)
for each (d − 1)-simplex σ ∈ DT(S)
    Compute λ-interval I(σ)
for each vertex v ∈ S
    GabrielSimplices_v = ∅
    for each σ ∈ DT(S) incident to v
        if upper λ-interval bound of σ equals 1
            Insert σ in GabrielSimplices_v
    ChosenSimplices_v = ∅
    while ChosenSimplices_v ⊉ umbrella at v
        Choose σ_min ∈ GabrielSimplices_v with minimal lower λ-interval bound
        Delete σ_min in GabrielSimplices_v
        Insert σ_min in ChosenSimplices_v
    for each σ ∈ ChosenSimplices_v
        if σ ∉ umbrella at v
            Delete σ in ChosenSimplices_v
return ⋃_{v∈S} ChosenSimplices_v
```

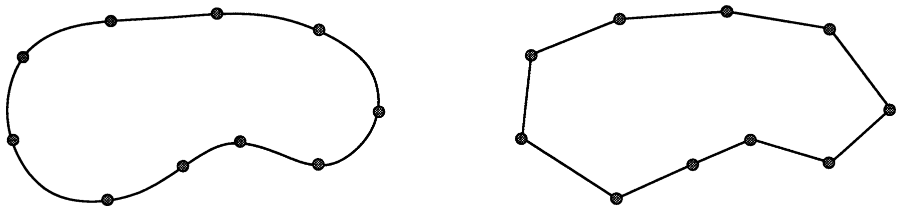

Fig. 2. A sample S from a curve and the correct polygonal reconstruction $P(S)$ given by UMBRELLAFILTER.

First the Delaunay triangulation and the λ-intervals are computed (lines 1–3). Based on this, an optimal umbrella is selected at each vertex v (lines 4–16) in the following way.

Determine the Gabriel simplices at v, namely the simplices whose upper λ-interval bound equals 1. From those, successively choose the Gabriel simplex with minimal lower λ-interval bound until the chosen simplices contain an umbrella (lines 9–13). Delete all chosen simplices at vertex v that do not belong to this umbrella (lines 14–16).

Finally, the algorithm returns the union of all chosen simplices (line 17).

Note that the operations on $\mathit{GabrielSimplices}_v$ in lines 8 and 11–12 can be implemented efficiently using a priority queue [11]. The umbrella checks in the lines 10 and 15 are discussed in the following subsections.

We observed that the algorithm UMBRELLAFILTER yields good results for well sampled smooth surfaces in two and three dimensions. Unfortunately, its output need not be topologically correct. In undersampled or non-smooth parts of a surface the umbrellas chosen at the vertices can conflict. At such vertices the umbrella condition of Definition 3.1 is violated. We show in Section 3.2 how such conflicts can be resolved.

3.1. *The two dimensional case*

A hypersurface in two dimensions is a simple closed curve. The *correct reconstruction* $P(S)$ of a curve from a finite sample S is the polygon, that connects the sample points in exactly the same way the points are connected along the curve (see Fig. 2). For the higher dimensional reconstruction problem we lack such a concise notion of correctness. That is, in contrast to its higher dimensional analogs, the curve reconstruction problem is not ill posed.

In two dimensions the umbrella condition reduces to two incident edges at each sample point, i.e. the algorithm UMBRELLAFILTER simply chooses for every point in S the two incident edges of the Gabriel graph with smallest lower λ-interval bound.

The algorithm UMBRELLAFILTER is a reconstruction scheme for a certain class of curves, i.e. for this class of curves there exists a finite sampling density such that for all samples S with larger sample density the algorithm UMBRELLAFILTER yields the correct reconstruction of the curve.

Before we can prove this we have to introduce some further notions. A *curve* γ is a collection of compact connected subsets of $\mathbb{R}^d$ which are pairwise disjoint and are either homeomorphic to the compact unit interval [0, 1] or to the unit circle $\mathbb{S}^1$. This definition is quite narrow but includes all curves considered in curve reconstruction so far. See Falconer [17] for a modern treatment of general curves. In this section we deal only with curves that are hypersurfaces, i.e. a curve consists only of one connected component which is homeomorphic to $\mathbb{S}^1$, but in the appendix we need the wider definition.

If the curve consists of only one connected component a *sample* of a curve is a finite sequence of points from the curve. We can define an order on the points by using an order of the points along the curve. To assign the notion of density to a sample we borrow the following definitions from [4]. The *medial axis* of a curve $\gamma \subset \mathbb{R}^2$ is the closure of the set of points that have more than one closest point on γ. The *local feature size* $f(p)$ at a point $p \in \gamma$ is the smallest distance from p to the medial axis. A finite point set $S \subset \gamma$ is called an ε-*sample* of a curve γ, if every point $p \in \gamma$ has a sample point $s \in S$ within distance of $\varepsilon f(p)$. This definition of sampling density adapts nicely to features of the curve, i.e. in regions of high curvature need to be more sample points than in regions with less curvature. Thus, an ε-sample need not be uniform. The disadvantage of this definition is that there is no ε-sample for non-smooth curves. Let p be a point of a non-smooth curve $\gamma \subset \mathbb{R}^d$ at which no tangent exists. The medial axis of the curve γ comes infinitely close to p. Hence, every ε-sample of γ must have infinitely many sample points in every neighborhood of p in order to fulfill the ε-sample condition, but by definition a sample has to be finite. Since we also want to include non-smooth curves in our discussion, we give up the non-uniformity property of an ε-sample and define an ε-sample instead as follows. A finite point set $S \subset \gamma$ is called an ε-sample of a curve γ, if every point $p \in \gamma$ has a sample point $s \in S$ within distance of ε. We refer to the first definition of ε-samples as non-uniform ε-samples.

The quantity

$$\varepsilon(S) = \sup_{p\in\gamma} \min_{s\in S} |s - p|$$

is a measure for the density of a sample S of the curve γ.

Finally, we introduce the notion of *regularity* of a curve. Let $\gamma : [0, 1] \to \mathbb{R}^d$ be a local parameterization of a curve and let

$$T = \{(t_1, t_2)\colon\ t_1 < t_2, t_1, t_2 \in [0, 1]\}$$

and

$$\tau : T \to \mathbb{S}^1, \qquad (t_1, t_2) \mapsto \frac{\gamma(t_1) - \gamma(t_2)}{|\gamma(t_1) - \gamma(t_2)|}.$$

The curve is called left (right) regular at $\gamma(t_0)$ with left tangent $\mathrm{l}(\gamma(t_0))$ or right tangent $\mathrm{r}(\gamma(t_0))$, if for every sequence (ξ_n) in T which converges from left (right) to (t_0, t_0) in closure(T) the sequence $\tau(\xi_n)$ converges to $\mathrm{l}(\gamma(t_0))$ or $\mathrm{r}(\gamma(t_0))$, respectively.

A curve is *semi regular* if it is left and right regular at all its points. It is *regular* if it is semi regular and the left and right tangents coincide at all its points. We call a curve *benign* if it is semi regular and at no point of the curve the left and the right tangent point in exactly opposite directions.

Left and right regularity in a point have a simple geometric interpretation, which we give here for the case of left regularity.

Lemma 3.1. *Let the curve γ be left regular in the point $s \in \gamma$. Let (p_n), (q_n) and (r_n) be sequences of points from γ, that converge to s from the left, such that $p_n < q_n < r_n$ for all $n \in \mathbb{N}$ in an order locally around s along the curve γ. Let α_n be the angle at q_n of the triangle with vertices p_n, q_n and r_n. Then the sequence (α_n) of angles converges to π.*

Proof. If we make use of a local parameterization of the curve γ which we also denote by γ for simplicity. The sequences $(\gamma^{-1}(p_n))$, $(\gamma^{-1}(q_n))$ and $(\gamma^{-1}(r_n))$ converge from left to $\gamma^{-1}(s)$. Thus by our definition of left regularity the three oriented secants $\overrightarrow{p_n q_n}$, $\overrightarrow{q_n r_n}$ and $\overrightarrow{p_n r_n}$ have to point asymptotically in the direction of the left tangent $1(s)$. Hence,

$$\lim_{n\to\infty} \alpha_n = \pi. \qquad \square$$

The algorithm UMBRELLAFILTER is a reconstruction scheme for regular curves in the plane, which are homeomorphic to $\mathbb{S}^1$.

Theorem 3.1. *Let γ be a regular curve in $\mathbb{R}^2$ which is homeomorphic to $\mathbb{S}^1$ then there exists $\varepsilon > 0$ such that for all samples S with $\varepsilon(S) < \varepsilon$ the algorithm* UMBRELLAFILTER *yields the correct reconstruction $P(S)$.*

Proof. The proof of this theorem is an immediate consequence of Lemma 3.2 and Lemma 3.3 which we will prove next. $\square$

Lemma 3.2. *Let γ be a regular curve in $\mathbb{R}^2$ which is homeomorphic to $\mathbb{S}^1$ and let (S_n) be a sequence of samples from γ with $\lim_{n\to\infty} \varepsilon(S_n) = 0$. For every two sequences (p_n), (q_n) with $p_n, q_n \in S_n$ it holds:*

(1) *It exists a sampling sensity $\varepsilon > 0$ such that for all samplings S_n with $\varepsilon(S_n) < \varepsilon$ and all edges $\overline{p_n q_n}$ which belong to the correct reconstruction the upper λ-interval bound equals 1, i.e.,*

$$\overline{p_n q_n} \in P(S_n) \quad \Longrightarrow \quad I(\overline{p_n q_n}) = 1 \quad \textit{for } n \textit{ large enough.}$$

(2) *If $\overline{p_n q_n}$ does not belong to the correct reconstruction $P(S_n)$, either the upper λ-interval bound does not converge to 1 or the lower λ-interval bound does not converge to 0, i.e.,*

$$\overline{p_n q_n} \notin P(S_n) \quad \Longrightarrow \quad \begin{array}{l} \textit{either } \limsup \sup I(\overline{p_n q_n}) < 1 \\ \textit{or } \liminf \inf I(\overline{p_n q_n}) > 0. \end{array}$$

Proof. (1) In [14] it is shown that for sufficiently dense samples the correct reconstruction is a subgraph of the Gabriel graph.

(2) Assume the contrary. By turning to appropriate subsequences we can assume without loss of generality that there exist two sequences (p_n) and (q_n) with the following properties:

(a) $\overline{p_n q_n} \notin P(S_n)$ for all $n \in \mathbb{N}$.
(b) $\lim_{n\to\infty} \sup I(\overline{p_n q_n}) = 1$.
(c) $\lim_{n\to\infty} \inf I(\overline{p_n q_n}) = 0$.
(d) $\lim_{n\to\infty} p_n = p \in \gamma$ and $\lim_{n\to\infty} q_n = q \in \gamma$ (by the compactness of γ).

We distinguish two cases: (1) $p = q$ and (2) $p \neq q$.

First case. Assume $p_n < q_n$ locally around p for all $n \in \mathbb{N}$ in the order along γ. By property (a) there has to exist a sequence (r_n) of sample points $r_n \in S_n$ with $p_n < r_n < q_n$ locally around p. Consider the triangles with corner points p_n, q_n and r_n. By the regularity of γ in p the sequence (α_n) of angles at the corner points r_n has to converge to π. Let α_n' and β_n be the angles opposite to the edge $\overline{p_n q_n}$ in the Delaunay triangulation of S_n. We can assume that r_n and the sample point corresponding to α_n lie on the same side of $\overline{p_n q_n}$. It follows that $\alpha_n \leqslant \alpha_n'$ and $\lim_{n\to\infty} \alpha_n' = \pi$. The Delaunay condition $\beta_n \leqslant \pi - \alpha_n'$ implies that the sequence (β_n) has to converge to zero. Hence,

$$\lim_{n\to\infty} \sup I(\overline{p_n q_n}) = \lim_{n\to\infty} \max\{\sin(\alpha_n'), \sin(\beta_n)\} = 0,$$

which contradicts property (b).

Second case. We show that in this case γ cannot be regular at the points p and q. Let h be the line through the points p and q. This line partitions $\mathbb{R}^2$ in two halfspaces. By property (c) the curve γ has to lie completely in one of these halfspaces. Let b be the open ball with diameter $|p-q|$ which has p and q in its boundary. By condition (b) the ball b cannot contain any point of γ. Let (r_n) and (s_n) be sequences of sample points $r_n, s_n \in S_n$ with

$$\lim_{n\to\infty} r_n = \lim_{n\to\infty} s_n = p$$

and $r_n < p < s_n$ locally around p in the order along γ. Consider the triangles with corner points r_n, p and s_n and the sequence (α_n) of angles at the corner point p. By construction is

$$\limsup \alpha_n \leqslant \frac{\pi}{2},$$

which is a contradiction to the regularity of γ in p. An analog reasoning shows that γ cannot be regular in q neither. □

The next lemma is concerned with the class of benign curves.

Lemma 3.3. *Let γ be a benign curve in $\mathbb{R}^2$, which is homeomorphic to $\mathbb{S}^1$ and let (S_n) be a sequence of samples from γ with $\lim_{n\to\infty} \varepsilon(S_n) = 0$. For every two sequences (p_n), (q_n) with $p_n, q_n \in S_n$ one finds: If $\overline{p_n q_n}$ belongs to the correct reconstruction $P(S_n)$, the lower λ-interval bound converges to* 0, *i.e.,*

$$\overline{p_n q_n} \in P(S_n) \quad \Longrightarrow \quad \lim_{n\to\infty} \inf I(\overline{p_n q_n}) = 0.$$

Proof. Assume the contrary. That is, there exist two sequences (p_n), (q_n) with $p_n, q_n \in S_n$ and $\overline{p_n q_n} \in P(S_n)$ such that

$$\limsup \inf I(\overline{p_n q_n}) > 0.$$

By turning to an appropriate subsequence we can assume that

$$\lim_{n\to\infty} \inf I(\overline{p_n q_n}) = c > 0.$$

Observe that the edges $\overline{p_n q_n}$ cannot be edges of the convex hull of S_n, because for convex hull edges e we have $\inf I(e) = 0$. Furthermore, we can assume, using the compactness of γ and $\lim_{n\to\infty} \varepsilon(S_n) = 0$, that

$$\lim_{n\to\infty} p_n = \lim_{n\to\infty} q_n = p \in \gamma.$$

We will show in an appendix that for sufficiently dense samples the correct reconstruction is a subgraph of the Delaunay graph of the sample points. Hence, for large n the edge $\overline{p_n q_n}$ is an edge of the Delaunay graph, which has two incident triangles with vertices in S_n. Let r_n and s_n be the vertices opposite to the edge $\overline{p_n q_n}$ in these triangles.

From our assumptions we find for the sequence (α_n) of angles at the vertices r_n,

$$\limsup \sin \alpha_n \geqslant c.$$

Analogously we find for the sequence (β_n) of angles at the vertices s_n,

$$\limsup \sin \beta_n \geqslant c.$$

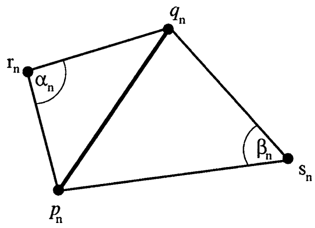

Fig. 3. The two triangles incident to the edge $\overline{p_n q_n}$.

By turning to appropriate subsequences we can assume that

$$\lim_{n\to\infty} \sin\alpha_n \geqslant c \quad \text{and} \quad \lim_{n\to\infty} \sin\beta_n \geqslant c. \tag{1}$$

We find for the diameters $\operatorname{diam}(p_n, q_n, r_n)$ and $\operatorname{diam}(p_n, q_n, s_n)$ of the unique balls through the points p_n, q_n and r_n or p_n, q_n and s_n, respectively,

$$\lim_{n\to\infty} \operatorname{diam}(p_n, q_n, r_n) = \lim_{n\to\infty} \frac{|p_n - q_n|}{\sin\alpha_n} = 0,$$
$$\lim_{n\to\infty} \operatorname{diam}(p_n, q_n, s_n) = \lim_{n\to\infty} \frac{|p_n - q_n|}{\sin\beta_n} = 0.$$

That is,

$$\lim_{n\to\infty} r_n = \lim_{n\to\infty} s_n = p.$$

Assume that in p the left tangent and the right tangent coincide, i.e. in p exists a unique tangent. Without loss of generality we can assume that $p_n < q_n < r_n$ for all $n \in \mathbb{N}$ in the order along γ locally around p. Consider the triangle with vertices p_n, q_n and r_n. From the definition of regularity the sequence (α_n) of angles converges to zero, which is a contradiction to the inequalities (1). Thus, it suffices to consider the case that in p the left and right tangents do not coincide.

By turning to appropriate subsequences one can consider without loss of generality two cases:
(1) $p_n < p < q_n$ along γ for all $n \in \mathbb{N}$,
(2) $p_n, q_n \leqslant p$ or $p \leqslant p_n, q_n$ along γ for all $n \in \mathbb{N}$.

First case. Let (h_n) be the sequence of lines through the points p_n and q_n. Since the sequences (r_n) and (s_n) both converge to p we find for sufficiently large $n \in \mathbb{N}$ that the points r_n and s_n lie both in the half space with boundary h_n that contains the point p. But this is impossible in a Delaunay triangulation.

Second case. Without loss of generality we assume that $p \leqslant p_n, q_n$ along γ for all $n \in \mathbb{N}$.

Now assume that $p \leqslant r_n$ or $p \leqslant s_n$ along γ for arbitrary large n. From the existence of the right tangent in p we find that the sequence (α_n) of angles or the sequence (β_n) has a subsequence that has to converge to zero. That is a contradiction to the inequalities (1).

We are left with the case that there exists $N \in \mathbb{N}$ such that $r_n, s_n < p$ for all $n \geqslant N$. Consider the sequence (h_n) of lines through the points p_n and q_n. This sequence converges to the line defined by the right tangent at p. Since $\angle(\mathrm{l}(p), \mathrm{r}(p)) < \pi$ and the sequences (r_n) and (s_n) both converge to p we find for large n that the points r_n and s_n have to lie both on the same side of the line h_n. Again, this is impossible in a Delaunay triangulation. $\square$

Table 1

	$e \in P(S)$	$e \notin P(S)$
Regular curve	$\lambda_0 \to 0$ and $\lambda_1 = 1$	$\lambda_0 \nrightarrow 0$ or $\lambda_1 \neq 1$
Benign curve	$\lambda_0 \to 0$	no property known

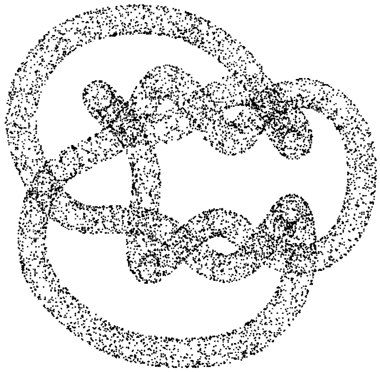

Fig. 4. KNOT (10000 points, non-uniform with some noise).

Let $I(e) = [\lambda_0, \lambda_1]$ be the λ-interval of an edge e in the Delaunay triangulation of a sample S. The statements of Lemmas 3.2 and 3.3 are summarized in Table 1 (the limits are taken with respect to increasing sampling density).

In the appendix we show that the class of benign curves is exactly the class of curves, for which the correct reconstruction can be found in the Delaunay triangulation for dense samples. Unfortunately, the algorithm UMBRELLAFILTER is not capable to reconstruct the entire class of benign curves.

3.2. The three-dimensional case

In three dimensions S is a finite sample from a compact closed surface embedded in $\mathbb{R}^3$. Fig. 4 shows an example. In this case we are not able to provide theoretical guarantees for the algorithm UMBRELLAFILTER as we do for the two dimensional case. But we observe that it gives good results in practice which are well suited for a postprocessing step we are going to describe later.

The algorithm UMBRELLAFILTER now chooses for each point $v \in S$ a set of triangles incident to v, which is topologically equivalent to a closed disk. To implement the umbrella check for a vertex v (line 10 of the algorithm) we construct a graph G_v with vertex set V_v, where V_v is the set of all vertices adjacent to v in the Gabriel complex. Each time a triangle with vertices v, v_1, v_2 is added to $\mathit{ChosenSimplices}_v$, we connect the vertices v_1 and v_2 in G_v by an edge. Hence, an umbrella at v corresponds to a cycle in G_v (for an example see Fig. 5).

To find a cycle in an undirected graph we start a depth-first search [11] on it. Now every back edge in the depth-first search tree closes a cycle and every cycle contains a back edge.

The output of the algorithm UMBRELLAFILTER for the sample points of Fig. 4 is shown in Fig. 6. The reconstruction looks good, but a zoom shows that the surface is topologically incorrect at some vertices (see Fig. 6(b)).

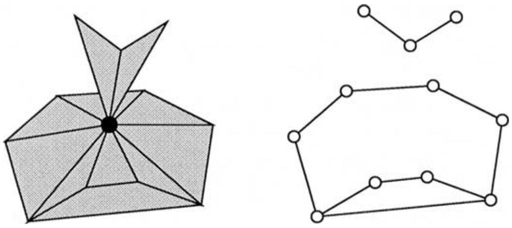

Fig. 5. The set of triangles incident to a vertex and the corresponding graph.

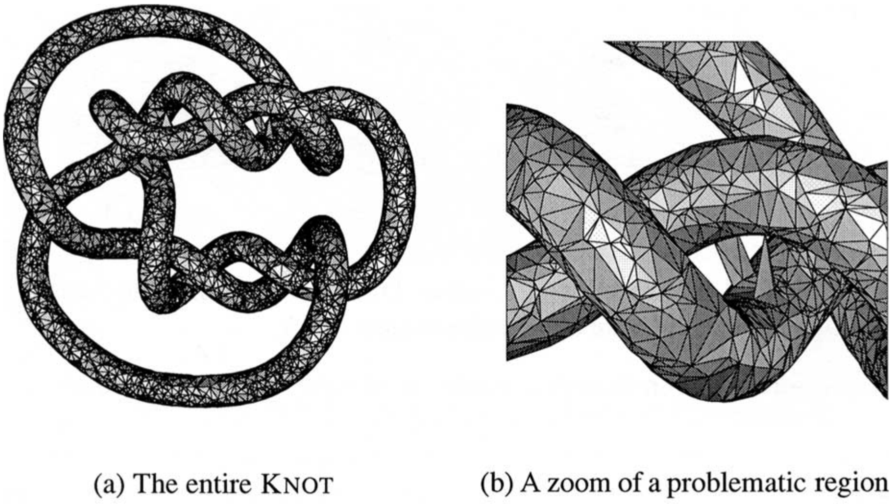

Fig. 6. Reconstruction of the KNOT with the algorithm UMBRELLAFILTER.

Our goal is to transform the output of the algorithm UMBRELLAFILTER into a topologically correct surface. Remember that every point of a two dimensional surface has a neighborhood homeomorphic to $\mathbb{D}^2$. In general, the output of the algorithm UMBRELLAFILTER is a two dimensional simplicial complex, but not a surface. We are interested in the question when a simplicial complex actually is a surface.

Definition 3.2 (Surface complex). A two-dimensional surface complex S is the geometric realization of a two dimensional simplicial complex where:

(a) Every vertex is incident to a triangle.
(b) Every edge is incident to exactly two triangles.
(c) For every vertex v the set $T_v = \{t_1, \ldots, t_n\}$ of its incident triangles can be ordered in a cyclic manner, i.e. t_i and t_{i+1} share an edge for $i = 1, \ldots, n$ with $t_{n+1} := t_1$.

Observe that the set T_v of triangles in property (c) corresponds exactly to an umbrella at vertex v. In [23] is shown that indeed every point of a surface complex has a neighborhood homeomorphic to $\mathbb{D}^2$, i.e. at every vertex of a surface complex the umbrella condition is fulfilled. Hence Definition 3.2 is consistent with the definition of a surface complex in arbitrary dimension in Definition 3.1.

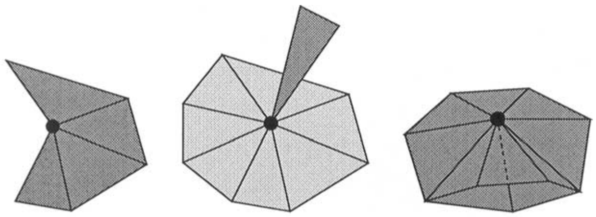

Fig. 7. Topological incorrectness at a vertex. Different types of triangles are indicated by dark shading. Observe that there are 3 umbrellas present in (c).

Topological clean up

At vertices where the umbrella condition is not fulfilled we distinguish 3 types of triangles indicating topological incorrectness. A triangle t is called *type 1,* if there is a vertex v incident to t and no umbrella at v (see Fig. 7(a)). A triangle t is called *type 2,* if there is a vertex v incident to t and at least one umbrella at v, but t is not contained in any umbrella at v (see Fig. 7(b)). Finally, a triangle t is called *type 3,* if there is a vertex v incident to t and at least two umbrellas at v and at least one of them contains t (see Fig. 7(c)).

We want to clean up the Gabriel complex avoiding triangles of type 1–3. At first we simply delete all triangles of type 2 and type 3 and all triangles becoming type 2 or type 3 thereby. It is important to note that the type of a triangle depends on the vertex. A triangle can possibly have different types at its three distinct vertices. A triangle of types 2 or 3 at vertex v is deleted, even though it might be of type 1 at its other vertices.

Deleting type 2 triangles yields vertices where each incident triangle is part of an umbrella. Deleting triangles of type 3 makes the umbrella at each vertex unique. We delete triangles of type 3 in reverse order of the lower bounds of their λ-intervals. The intuition behind this is that triangles of the reconstruction tend to have small lower λ-interval bounds. Note that we cannot successively delete type 1 triangles, because a continuous deletion of this triangles generates new type 1 triangles and possibly deletes all triangles.

The check which triangles are part of an umbrella can be accomplished by depth-first search on the corresponding graph like the umbrella check explained above.

Our deletion step yields vertices with exactly one incident umbrella, and vertices without any incident umbrella, i.e. triangles of type 1. A subset of the set of vertices without an incident umbrella makes up a *hole* H, if it is connected by edges with the following property. The edge has exactly one incident triangle and this is of type 1. Hence, all vertices of the boundary of the 'hole' are contained in the set H. In addition to that, a vertex also belongs to H, if it is connected to H by a triangle, that has been deleted during the topological clean up. This is necessary as the deletion of triangles possibly disconnects 'inner' vertices from the boundary of the 'hole'. Fig. 8 shows a hole in the surface of the example KNOT after this reduction step.

Establishing closed surfaces

Next we want to close all holes by extending the surface through it. Let T_H be the set of all triangles of the Delaunay triangulation of S having all their vertices in a hole H. We can assume that the output of

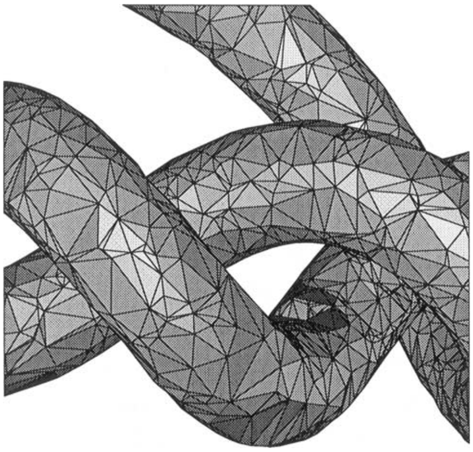

Fig. 8. A zoom after the topological clean up.

the algorithm UMBRELLAFILTER after the clean up step, together with the triangles in the sets T_H for all holes H, contain a topologically correct surface. We propose a technique for extracting a topologically correct surface from a simplicial complex. We formulate the topological surface conditions as linear inequalities in such way, that a solution with integer values specifies a topologically correct surface. This surface can be seen as a feasible integer solution of a linear program. It turns out that a simplicial complex that satisfies all inequalities is a surface complex.

Definition 3.3 (Constrained complex). Given a two-dimensional finite simplicial complex K with vertices V, edges E and triangles T. Let $T_v \subset T$ denote the triangles incident to a vertex $v \in V$. Similarly, $T_e \subset T$ denotes the set of triangles incident to an edge $e \in E$. We associate a variable x_t with each triangle $t \in T$. The set of triangles for which the corresponding variables are set to 1 in an integer solution of the following set of inequalities is called a constrained complex of K.

$$\forall t \in T: \qquad 0 \leqslant x_t \leqslant 1, \tag{2}$$

$$\forall e \in E: \qquad \sum_{t \in T_e} x_t \leqslant 2, \tag{3}$$

$$\forall e \in E,\ \forall t \in T_e: \qquad x_t - \sum_{t' \in T_e,\ t' \neq t} x_{t'} \leqslant 0, \tag{4}$$

$$\forall v \in V: \qquad \sum_{t \in T_v} x_t \geqslant 1, \tag{5}$$

$$\forall v \in V \qquad \forall \text{ umbrellas } U_1, U_2 \subset T_v,\ U_1 \cap U_2 \neq \emptyset:$$

$$\sum_{t \in U_1} x_t + \sum_{t \in U_2} x_t \leqslant |U_1| + |U_2| - 1. \tag{6}$$

Observe the following. If a constrained complex K_c of a simplicial complex K exists, then K_c contains all vertices of K, because of the inequalities (5). In general, there need not be a unique constrained subcomplex. There are special cases where a constrained complex is unique, e.g. a constrained complex of a surface complex K is always the surface complex K itself, i.e. all variables associated with the triangles of K equal 1.

We prove that a constrained complex always is a surface complex.

Theorem 3.2. *Every constrained complex is a surface complex.*

Proof. We have to show that a constrained complex of a simplicial complex has properties (a)–(c) of a surface complex, see Definition 3.2.

Since a constrained complex only chooses triangles from the initial simplicial complex it can not contain vertices that are not incident to a triangle, i.e. property (a) of a surface complex also holds for a constrained complex.

For the same reason, every edge in the constrained complex is incident to at least one triangle. Inequalities (3) forbid more than two incident triangles at an edge and inequalities (4) forbid edges with exactly one incident triangle. Hence, every edge is incident to exactly two triangles, which is property (b) of a surface complex.

Next, we construct a subset U_1 of the triangles T_v incident to a vertex v that fulfills property (c). We start with a triangle t_1 (which exists because of inequality (5)). Property (b) assures, that there is a triangle $t_2 \in T_v$ incident to t_1 at an edge and a triangle $t_3 \in T_v$ incident to t_2 at the other edge incident to v, and so on. We reach t_1 again after finitely many steps, because T_v is a finite set. The set $U_1 := \{t_1, \ldots, t_n\}$ fulfills property (c), i.e. U_1 is an umbrella. Assume, property (c) does not hold and there is a triangle $t \in T_v$ with $t \notin U_1$. Starting at t, we can construct an umbrella U_2 in the same way we constructed U_1. Because of property (b), U_2 shares no triangle with U_1. This is a contradiction to inequalities (6). □

In our application the initial complex, for which we want to compute a constrained subcomplex, is the output of the algorithm UMBRELLAFILTER after the topological clean up, augmented by all triangles from the Delaunay complex having all their vertices in a hole H. The inequalities (2)–(6) can be generated efficiently by iterating over all triangles incident to an edge or a vertex, respectively. In general, integer linear programming is a difficult task. Nevertheless, we are interested only in a feasible solution for the inequalities (2) to (6) and our initial complex is a good approximation to the resulting constrained complex. Thus, the constrained complex can be computed by available LP solvers, e.g. [12].

Fig. 9 shows the correctly reconstructed example KNOT after applying the topological postprocessing. The surface is now topologically correct at every vertex.

4. Implementation and results

In two dimensions the algorithm UMBRELLAFILTER works also well in practice. An implementation in Java can be found at http://www.inf.ethz.ch/∼adamy/curve.html.

For the three dimensional case we implemented our algorithm using the C++ programming language. Our implementation is based on the Computational Geometry Algorithms Library CGAL [10], which includes fast and robust Delaunay triangulations for two and three dimensions. We used the commercial linear program solver CPLEX [12] that provides methods to find integer solutions for linear inequalities. All results are viewed and rendered by GEOMVIEW [18].

We tested our 3D-algorithm on several examples on a Sun Ultra 1 machine with a 143 MHz processor and 256 MByte memory. The outcome of our tests is pictured in Figs. 13 and 14. Additional information

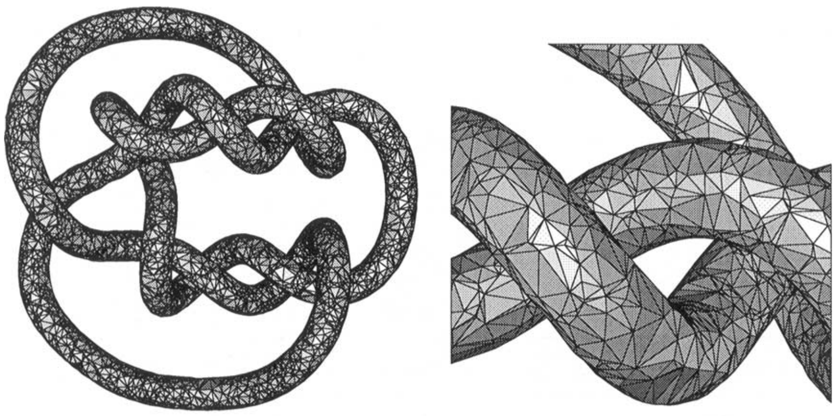

(a) The entire KNOT (b) A zoom

Fig. 9. The perfectly reconstructed KNOT.

is listed in Table 2. The left column of Fig. 13 presents two further examples for the output of the algorithm UMBRELLAFILTER. They show the quality of this algorithm. Table 2 summarizes more detailed information about the runtimes and the number of output triangles for the UMBRELLAFILTER algorithm and the topological postprocessing (including topological clean-up and LP-solving). The runtimes are fast, particularly compared to the CRUST algorithm [3,5].

Unfortunately, the output of the algorithm UMBRELLAFILTER without postprocessing is not topologically correct at every vertex. That can be easily seen by the following equation derived from Euler's formula, which is a necessary condition for a closed and triangulated surface:

$$\#\,\text{triangles} = 2 \cdot \#\,\text{vertices} + 4 \cdot (\text{genus} - 1), \tag{7}$$

where genus is 0 for all shown examples except the examples KNOT (genus $=$ 1) and 3HOLES (genus $=$ 3). The number of triangles given in Table 2 is slightly too large to fulfill this equation.

But we can enforce topologically correctness with our topological postprocessing step including LP-solving for all examples (except for the difficult DRAGON). For these examples the number of triangles after this step (see Table 2) equals exactly the number of triangles postulated in Eq. (7). The additional amount in runtime is a matter of seconds.

Problems occur with samples like the DRAGON. In the output of the algorithm UMBRELLAFILTER there are some regions that we have to repair with the linear programming approach, which are quite large and correspond to highly non-smooth or undersampled parts of the surface. While for moderately sized problematic regions a feasible integer solution for the inequalities (2)–(6) in Section 3.2 can be found very fast, for some difficult regions the problem might take a long time or be infeasible.

However, the zoom in Fig. 14(f) shows how good our two approaches collaborate even in non-smooth and undersampled parts of the surface. For this example we encounter only one region that blows up the running time.

Table 2
Performance of our algorithm for different objects

Object	Number of points	UMBRELLAFILTER algorithm: Number of triangles	UMBRELLAFILTER algorithm: Runtime (sec)	After topological postprocessing: Number of triangles	After topological postprocessing: Total runtime (sec)
KNOT	10000	20396	33	20000	42
3HOLES	4000	8108	10	8008	13
BUNNY	35948	73040	121	71892	169
MANNEQUIN	12772	25646	29	25540	42
FOOT	20021	40180	48	40038	62
CLUB	16585	33308	69	33166	83
OILPUMP	30937	62873	87	61870	111
DRAGON	25010	51521	60	50026	521

We conclude that our approach in three dimensions is split two steps, the algorithm UMBRELLAFILTER and a topological postprocessing. They are to a large extent independent of each other, but nevertheless work together very well.

The topological methods we presented should be useful also for other algorithms, e.g. [3,6]. They build on the output of these algorithms and turn it into a topologically correct surface. Especially the techniques from linear programming can be a very powerful tool.

It is a topic of future research to fully exploit this power.

Appendix A. On the class of curves that can be reconstructed using the Delaunay triangulation

We show that there exists a finite sampling density such that the correct reconstruction of a benign curve is always a subgraph of the Delaunay triangulation. Furthermore, we give an example that shows the necessity of the assumption that the curve is benign. It is interesting to note that the necessary and sufficient regularity assumptions are exactly the same as for the Traveling Salesman Tour based reconstruction [19]. In the proof we will make use of the following lemma.

Lemma A.1. *Let (p_n), (q_n) and (r_n) be three sequences in $\mathbb{R}^d$, which all converge to the same point p. Let d_n be the diameter of the unique circle through the points p_n, q_n, r_n. If there are no subsequences of (p_n), (q_n), (r_n) such that p_n, q_n, r_n are asymptotically collinear, then* $\lim_{n\to\infty} d_n = 0$.

Proof. Consider the triangle with vertices p_n, q_n, r_n and inner angles $\alpha_n, \beta_n, \gamma_n$. Let $\delta_n = \max\{\alpha_n, \beta_n, \gamma_n\}$ and let e_n be the edge opposite to δ_n. The diameter d_n can be computed as follows:

$$d_n = \frac{\text{length}(e_n)}{\sin(\delta_n)}.$$

By our assumptions we find

$$\lim_{n\to\infty} \text{length}(e_n) \leqslant \lim_{n\to\infty} \max\{|p_n - r_n|, |p_n - q_n|, |q_n - r_n|\} = 0$$

and $\limsup \delta_n < \pi$. By construction we have $\delta_n \geqslant \pi/3$ for all $n \in \mathbb{N}$. Altogether this implies $\lim_{n\to\infty} d_n = 0$. □

The *1-skeleton* of the Delaunay triangulation is the collection all one dimensional Delaunay simplices. We say that a graph on a finite set $S \subset \mathbb{R}^d$ is a subgraph of the Delaunay triangulation of S, if it is embedded in the 1-skeleton of the Delaunay triangulation.

Theorem A.1. *For every benign curve γ there exists an $\varepsilon > 0$ such that for all samples S of γ with $\varepsilon(S) < \varepsilon$ the correct reconstruction of γ from S is a subgraph of the Delaunay triangulation of S.*

Proof. The proof is done by contradiction. Assume the theorem is not true. Then there exists a benign curve and sequence of samples (S_n) with $\lim_{n\to\infty} \varepsilon(S_n) = 0$ and $p_n, q_n \in S_n$ such that p_n and q_n are connected along the curve γ, but the edge $\overline{p_n q_n}$ is not a Delaunay edge. We show that the existence of any such sequence necessarily leads to a contradiction to the regularity of the curve γ.

We start by showing that there exists a subsequence of (S_n) such that the two sequences (p_n) and (q_n) both converge to the same point p on γ. Later we will show that γ cannot fulfill our regularity assumptions in p, which is the contradiction we are looking for.

Assume such a subsequence does not exist. By the compactness of γ we can assume that (p_n) converges to $p \in \gamma$ and (q_n) converges to $q \in \gamma$. Now our assumption just states that $|p - q| \geqslant c > 0$. On γ there has to exist a point r between p and q along γ with $|r - p| \geqslant c/2$ and $|r - q| \geqslant (c/2)c$. By our sampling condition we find $r_n \in S_n$ with $|r - r_n| < \varepsilon(S_n)$ for every $n \in \mathbb{N}$, i.e. the sequence (r_n) converges to r. That is impossible for curves without branching points. Hence we can assume that (p_n) and (q_n) converge to the same point p.

To make things easier we assume that p_n and q_n always belong to the component of γ containing p and that $p_n < q_n$ locally around p. This can always be achieved by switching to an appropriate subsequence.

Since γ is benign both left and right tangent have to exist at p. We consider two cases. Either the left and right tangent at p form an acute angle less than $\pi/2$ or they form an acute angle larger or equal to $\pi/2$.

We start with the first case. Let b_n be the open ball with diameter $d_n = |p_n - q_n|$ that has p_n and q_n in its boundary. Since we assume that the edge $\overline{p_n q_n}$ is not Delaunay, there exists a sample point r_n inside b_n, i.e. $r_n \in \text{closure}(b_n) \cap (S_n - \{p_n, q_n\})$, for all $n \in \mathbb{N}$. Without loss of generality assume that $q_n < r_n$ along γ. From $\lim_{n\to\infty} d_n = 0$ it follows that $\lim_{n\to\infty} r_n = p$. Consider the triangle with vertices p_n, q_n and r_n. From the law of cosines together with $|p_n - r_n| \leqslant |p_n - q_n|$, one finds for the angle α_n at q_n,

$$\cos(\alpha_n) = -\frac{|p_n - r_n|^2 - |p_n - q_n|^2 - |q_n - r_n|^2}{2|p_n - q_n||q_n - r_n|} \geqslant 0.$$

Thus, α_n has to be smaller or equal to $\pi/2$. But from our regularity assumption we get

$$\liminf \alpha_n > \frac{\pi}{2},$$

which yields a contradiction.

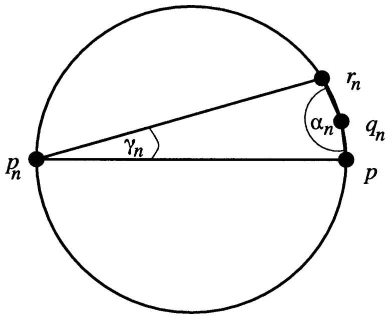

Fig. 10. The quadrilateral with vertices p_n, p, q_n and r_n which are asymptotically cocircular.

In the second case the left and right tangent at p form an acute angle larger or equal than $\pi/2$. In this case we can restrict ourselves to two subcases again by considering appropriate subsequences:
(1) $p_n < p < q_n$ along γ for all $n \in \mathbb{N}$,
(2) $p_n, q_n \leqslant p$ or $p \leqslant p_n, q_n$ along γ for all $n \in \mathbb{N}$.
Our goal is in either case to construct a contradiction to the assumption that the edge $\overline{p_n q_n}$ is not Delaunay.

We start with the first subcase. Let b_n be the smallest open ball which contains the points p_n, q_n and p in its boundary. Let d_n be the diameter of b_n. Since in p left and right tangent do not coincide, there are no subsequences of (p_n) and (q_n) such that p_n, q_n and p become collinear. Using Lemma A.1 this implies $\lim_{n\to\infty} d_n = 0$. By our assumption that the edge $\overline{p_n q_n}$ is not Delaunay there has to lie another sample point r_n in the closure of b_n. Without loss of generality we can assume that $q_n < r_n$ along γ and by moving r_n a little bit on γ that $r_n \in \partial b_n$. From $\lim_{n\to\infty} d_n = 0$ it follows that also $\lim_{n\to\infty} r_n = p$. Now consider the quadrilateral with vertices p_n, p, q_n and r_n. The points p_n, p, q_n and r_n are asymptotically cocircular since they all lie asymptotically in the plane spanned by $\{\mathrm{l}(p)$ and $\mathrm{r}(p)\}$. Let α_n be the angle at q_n and γ_n be the angle at p_n. From the right regularity of γ in p one has $\lim_{n\to\infty} \alpha_n = \pi$. Hence asymptotically the situation looks like the situation depicted in Fig. 10. Opposite angles in a cyclic quadrilateral always sum up to π. Since p_n, p, q_n and r_n are asymptotically cocircular this means $\lim_{n\to\infty}(\alpha_n + \gamma_n) = \pi$. Therefrom we get $\lim_{n\to\infty} \gamma_n = 0$, which implies

$$\lim_{n\to\infty} \angle\big(\overline{p_n q_n}, \mathrm{l}(p)\big) = 0.$$

Hence for large n the ball b'_n that we define next contains the point p. Let b'_n be the ball that has p_n and q_n in its boundary and its tangent hyperplane at q_n is orthogonal to the line l in $\operatorname{span}\{\mathrm{l}(p), \mathrm{r}(p)\}$ that halves the angle $\angle(\mathrm{l}(p), \mathrm{r}(p))$. For large n the situation in two dimensions is similar to the situation depicted in Fig. 11.

Let d'_n be the diameter of b'_n. Next we show that also $\lim_{n\to\infty} d'_n = 0$. Consider the line through the points p_n and p. This line intersects the boundary of the ball b'_n in the point p_n and in a second point p'_n. On this line p lies in between p_n and p'_n since b'_n contains p. Consider the triangle with corner points p_n, p'_n and q_n. All these points lie on the boundary of b'_n. Let α be the turning angle from $\mathrm{l}(p)$ to $\mathrm{r}(p)$. Since γ is benign we have $\alpha < \pi$. The angle in the triangle $p_n p'_n q_n$ at the point p'_n is by construction larger than $(\pi - \alpha)/2$. Altogether this implies

$$0 < \cos\left(\frac{\alpha}{2}\right) = \sin\left(\frac{\pi - \alpha}{2}\right) \leqslant \lim_{n\to\infty} \frac{|p_n - q_n|}{d'_n}.$$

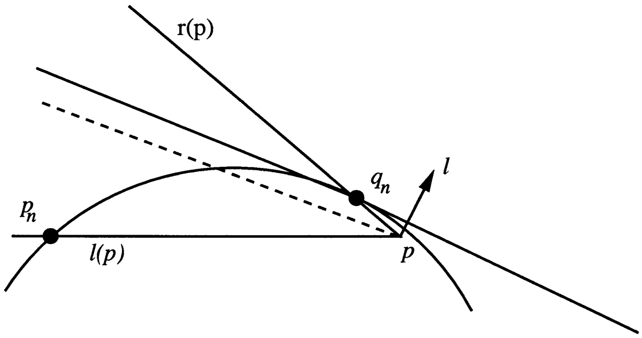

Fig. 11. Situation near the irregular point p.

Since $\lim_{n\to\infty} |p_n - q_n| = 0$, we find also for the diameters d'_n that

$$\lim_{n\to\infty} d'_n = 0.$$

By our assumption, that the edge $\overline{p_n q_n}$ is not Delaunay, there has to lie another sample point s_n in the closure of b'_n. Since $\lim_{n\to\infty} d'_n = 0$, we also have $\lim_{n\to\infty} s_n = p$. Next we consider the triangle with vertices p_n, q_n and s_n. Along γ we have that either $q_n < s_n$ or $s_n < p_n$. By turning once again to an appropriate subsequence we can assume that only one of these alternatives holds for all $n \in \mathbb{N}$.

If $q_n < s_n$, consider the triangle with vertices p, q_n and s_n. In the limit we find for the angle α_n at q_n that

$$\lim_{n\to\infty} \alpha_n \leqslant \pi - \frac{\pi - \alpha}{2} = \frac{\pi + \alpha}{2} < \pi,$$

because s_n has to lie on the same side of tangent plane of b'_n at q_n as the ball b'_n itself. By Lemma 3.1 this contradicts the right regularity of γ in p. If $s_n < p_n$, the same reasoning leads to a contradiction to the left regularity of γ in p.

It remains to discuss the second subcase. Assume $p_n, q_n \leqslant p$. The proof, if $p_n, q_n \geqslant p$, follows the same lines. Let l be the line in $\mathrm{span}\{\mathrm{r}(p), \mathrm{l}(p)\}$ that halves the angle $\angle(\mathrm{l}(p), \mathrm{r}(p))$. Let h be the hyperplane orthogonal to l that passes through p and let b_n be the open ball with $p_n, q_n \in \partial b_n$ and with diameter $d_n = |p_n - q_n|$. There are three possibilities:

(a) $\partial b_n \cap h = \emptyset$,

(b) $\partial b_n \cap h$ is a single point,

(c) $\partial b_n \cap h$ is a $(d-1)$-dimensional ball b'_n.

In case (c) we replace b_n by another ball. By continuity there exists a point $r_n \in b'_n$ such that in this point h is tangent to the smallest ball which contains the unique circle through the points p_n, q_n and r_n. Replace b_n by this ball.

Now we can treat all three cases (a)–(c) in the same way. Since p_n, q_n and r_n cannot have subsequences that become collinear by Lemma A.1, $\lim_{n\to\infty} d_n = 0$ still holds. The situation in two dimensions is similar to the situation depicted in Fig. 12. By the assumption that the edge $\overline{p_n q_n}$ is not Delaunay there has to lie another sample s_n in the closure of b_n. From $\lim_{n\to\infty} d_n = 0$ we also have $\lim_{n\to\infty} s_n = p$.

Let α denote again the turning angle from $\mathrm{l}(p)$ to $\mathrm{r}(p)$. Since the curve γ is benign we have $\alpha < \pi$. Along γ we have that either $p \leqslant s_n$ or $q_n < s_n < p$ or $s_n < p_n$. By turning to an appropriate subsequence we can assume that only one of these alternatives holds for all $n \in \mathbb{N}$.

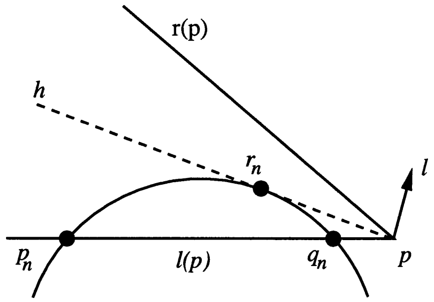

Fig. 12. Situation near the irregular point p.

If $p \leqslant s_n$, then

$$\lim_{n\to\infty} \angle\big(\overline{p_n q_n}, \mathrm{r}(p)\big) \geqslant \frac{\pi-\alpha}{2} > 0$$

in contradiction to the right regularity of γ in p.

If $q_n < s_n < p$ consider the triangle with vertices p_n, q_n and s_n. In the limit we find for the angle α_n at q_n that

$$\lim_{n\to\infty} \alpha_n \leqslant \pi - \frac{\pi-\alpha}{2} = \frac{\pi+\alpha}{2} < \pi,$$

because s_n lies on the same side of the tangent plane of b_n at q_n as the ball b_n itself and the tangent plane at q_n makes an acute angle larger $\pi/2$ with $\mathrm{l}(p)$. By Lemma 3.1 that is a contradiction to the left regularity of γ in p. In the same way we can construct a contradiction to the left regularity of γ in p if $s_n < p_n$.

We have shown that the assumption that there exists a sequence of samples (S_n) which become arbitrary dense in γ with $p_n, q_n \in S_n$ such that p_n and q_n are connected along γ, but the edge $\overline{p_n q_n}$ is not a Delaunay edge leads to a contradiction in any case, which proves the theorem. □

The following example shows that the conditions in Theorem A.1 are necessary. Let γ be the arc in the plane consisting of the unit interval on the x-axis and the graph of $y = x^2$ over this interval. That is,

$$\gamma : [0,1] \to \mathbb{R}^2, \qquad t \to \begin{cases} (1-2t, 0), & t \leqslant 1/2, \\ \big(2t-1, (2t-1)^2\big), & t > 1/2. \end{cases}$$

In every point of γ left and right tangents exist, but at the point $(0,0)$ the turning angle from the left tangent to the right tangent is π. Thus, the curve γ is not benign. For large n, the samples

$$S_n = \{p_n^1, p_n^2, p_n^3, p_n^4\} \cup \bigcup_{i=2}^{n} \left\{ \left(\frac{i}{n}, 0\right), \left(\frac{i}{n}, \frac{i^2}{n^2}\right) \right\},$$

with

$$p_n^1 = \left(\frac{1}{n}, 0\right), \quad p_n^2 = \left(\frac{1}{n^3}, \frac{1}{n^6}\right), \quad p_n^3 = \left(\frac{2}{n^3}, \frac{4}{n^6}\right), \quad p_n^4 = \left(\frac{1}{n^2}, \frac{1}{n^4}\right)$$

become arbitrary dense in γ. Let r_n be the radius of the unique circle through the points p_n^1, p_n^2 and p_n^3. Its easy to calculate that

$$\lim_{n\to\infty} r_n = \infty.$$

That is, if we extend γ to the half space $\{(x, y)\colon\ y < 0\}$ and take sample points in this half space, we find for large n by the open ball criterion for Delaunay edges that the edge $p_n^1 p_n^2$ cannot be a Delaunay edge. Therefore the conditions in Theorem A.1 are sufficient and necessary. □

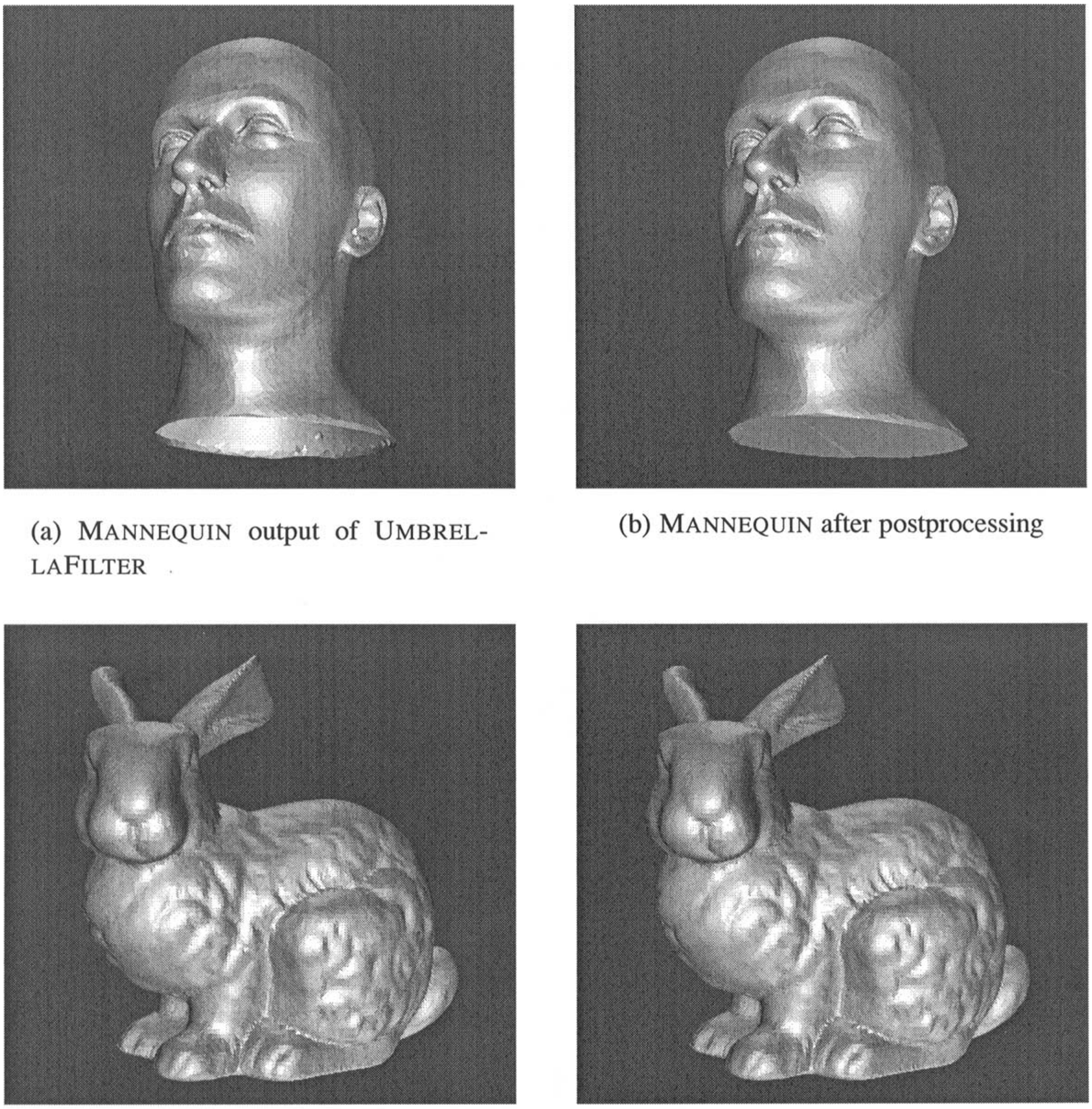

(a) MANNEQUIN output of UMBRELLAFILTER

(b) MANNEQUIN after postprocessing

(c) BUNNY output of UMBRELLAFILTER

(d) BUNNY after postprocessing

Fig. 13. Comparison between the output of UMBRELLAFILTER without (on the left) and with topological postprocessing (on the right).

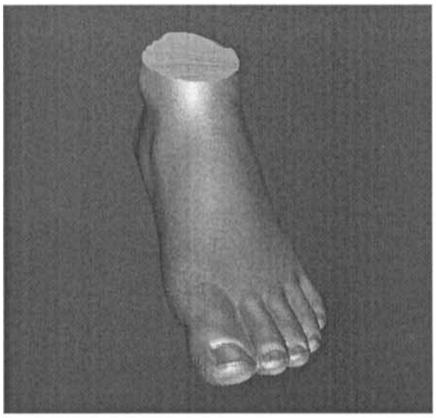

(a) FOOT

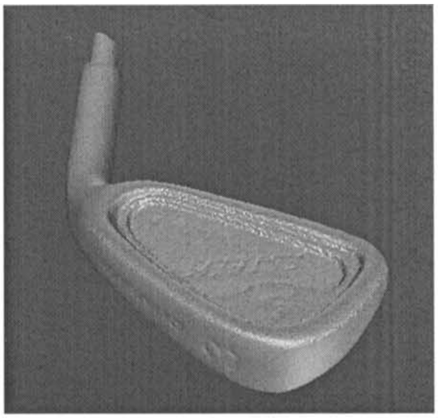

(b) CLUB

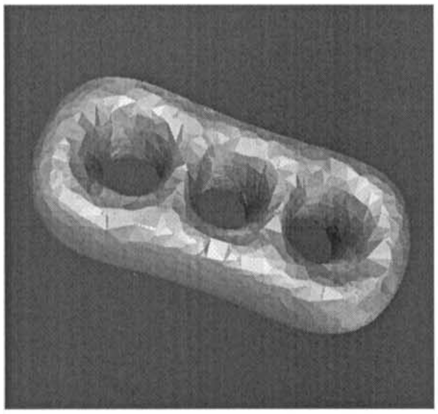

(c) 3HOLES

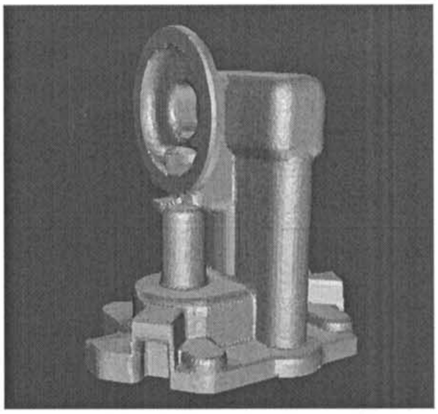

(d) OILPUMP

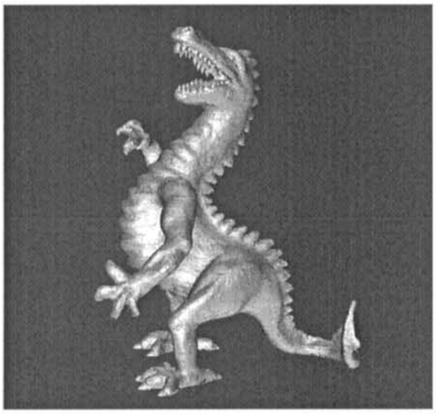

(e) DRAGON

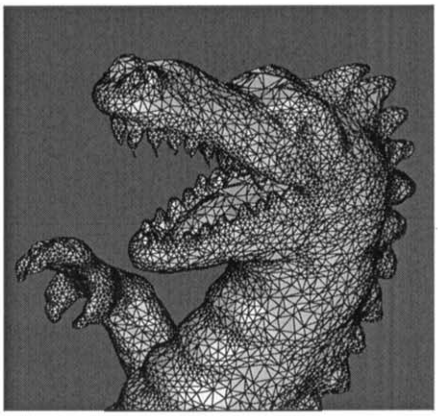

(f) Zoom of DRAGON

Fig. 14. More examples of the algorithm UMBRELLAFILTER with postprocessing.

References

[1] U. Adamy, J. Giesen, M. John, New techniques for topologically correct surface reconstruction, in: Proceedings of the 11th Annual IEEE Visualization Conference (VIS ’00), 2000, pp. 373–380.

[2] E. Althaus, K. Mehlhorn, TSP-based curve reconstruction in polynomial time, in: Proceedings of the 11th Annual ACM–SIAM Symposium on Discrete Algorithms (SODA ’00), 2000, pp. 686–695.

[3] N. Amenta, M. Bern, Surface reconstruction by Voronoi filtering, Discrete Comput. Geom. 22 (4) (1999) 481–504.

[4] N. Amenta, M. Bern, D. Eppstein, The crust and the β-skeleton: Combinatorial curve reconstruction, Graphical Models Image Process. 60 (2) (1998) 125–135.

[5] N. Amenta, M. Bern, M. Kamvysselis, A new Voronoi-based surface reconstruction algorithm, in: Proceedings of ACM SIGGRAPH 98, 1998, pp. 412–415.

[6] N. Amenta, S. Choi, T.K. Dey, N. Leekha, A simple algorithm for homeomorphic surface reconstruction, in: Proceedings of the 16th Annual ACM Symposium on Computational Geometry (SCG ’00), 2000, pp. 213–222.

[7] D. Attali, r-regular shape reconstruction from unorganized points, Computational Geometry 10 (1998) 239–247.

[8] C.L. Bajaj, E. Bernardini, G. Xu, Automatic reconstruction of surfaces and scalar fields from 3D scans, in: Proceedings of ACM SIGGRAPH 95, 1995, pp. 109–118.

[9] J.-D. Boissonnat, Geometric structures for three-dimensional shape representation, ACM Trans. Graphics 3 (4) (1984) 266–286.

[10] Computational Geometry Algorithms Library (CGAL), http://www.cgal.org.

[11] T.H. Cormen, C.E. Leiserson, R.L. Rivest, Introduction to Algorithms, MIT Press, Cambridge, MA, 1990.

[12] CPLEX, http://www.cplex.com.

[13] B. Curless, M. Levoy, A volumetric method for building complex models from range images, in: Proceedings of ACM SIGGRAPH 96, 1996, pp. 303–312.

[14] T.K. Dey, P. Kumar, A simple provable algorithm for curve reconstruction, in: Proceedings of the 10th Annual ACM–SIAM Symposium on Discrete Algorithms (SODA ’99), 1999, pp. 893–894.

[15] H. Edelsbrunner, D.G. Kirkpatrick, R. Seidel, On the shape of a set of points in the plane, IEEE Trans. Inform. Theory 29 (1983) 551–559.

[16] H. Edelsbrunner, E.P. Mücke, Three-dimensional alpha shapes, ACM Trans. Graphics 13 (1) (1994) 43–72.

[17] K.J. Falconer, The Geometry of Fractal Sets, Cambridge University Press, Cambridge, UK, 1985.

[18] Geomview, http://www.geom.umn.edu/software/geomview.

[19] J. Giesen, Curve reconstruction, the Traveling Salesman Problem, and Menger’s Theorem on length, in: Proceedings of the 15th Annual ACM Symposium on Computational Geometry (SCG ’99), 1999, pp. 207–216.

[20] H. Hoppe, T. DeRose, T. Duchamp, J. McDonald, W. Stuetzle, Surface reconstruction from unorganized points, Computer Graphics (Proceedings of SIGGRAPH92) 26 (2) (1992) 71–78.

[21] D.G. Kirkpatrick, J.D. Radke, A framework for computational morphology, Computational Geometry (1985) 217–248.

[22] M. Teichmann, M. Capps, Surface reconstruction with anisotropic density-scaled alpha shapes, in: Proceedings of the 9th Annual IEEE Conference on Visualization (VIS ’98), 1998, pp. 67–72.

[23] T. tom Dieck, Topologie, DeGruyter, Berlin, 1991.

[24] R.C. Veltkamp, The gamma-neighborhood graph, Computational Geometry 1 (1992) 227–246.